RSC Advances

PAPER

View Article Online
View Journal | View Issue

Cite this: *RSC Adv.*, 2021, **11**, 33408

Ferrocene-based conjugated microporous polymer and its multiwalled carbon nanotube composite for direct photocatalytic benzene hydroxylation to phenol

Zhongpeng Zhu, †[a] Long Pan,†[b] Zilu Liu,[b] Jie Zhao,*[a] Zhiping Tao*[a] and Yujian He[b]

Received 21st June 2021
Accepted 3rd October 2021

DOI: 10.1039/d1ra04810d

rsc.li/rsc-advances

Ferrocene is used as a catalytically active site and building block to construct a new conjugated microporous polymer (CMP), named **Fc-POP**. A corresponding carbon nanotube composite (**CNTs@Fc-POP**) with tubular structure was obtained through the π–π interaction between multi-walled carbon nanotubes (MWCNTs) and reactive molecules. This innovative modification method of carbon nanotubes provides a way to construct functionalized carbon materials. The two materials can achieve high conversion and selectivity of benzene hydroxylation to phenol under light irradiation using hydrogen peroxide (H_2O_2) as an oxidant. Due to the synergistic effect between the carbon nanotubes and the ferrocene group, the incorporation of MWCNTs can improve the yield of phenol significantly. This work explores a new photocatalytic system and expands the related photocatalytic application of CNTs.

Introduction

Phenol is an important chemical in industrial manufacturing, and has been applied in the production of plastics, fibers, medicines, rubber, dyes, *etc.*[1] Industrially, phenol is produced through the well-known three-step cumene process,[2] in which hazardous cumene peroxide and an almost equimolar amount of acetone are formed. Due to the low atom economy of the process, harsh experimental conditions and expensive equipment, direct oxidative hydroxylation of benzene to phenol using environmentally benign oxidants such as O_2,[3,4] NO_2 (ref. 5 and 6) and H_2O_2 (ref. 7) has received extensive research attention. The employment of H_2O_2 has achieved a green process, with water as the only byproduct. However, it is challenging to introduce the hydroxyl group directly onto the benzene ring. Due to the low reactivity of the sp^2 C–H bond, although almost all of the developed catalytic systems require elevated temperatures, the conversion efficiencies are still low. Another existing problem is that it is difficult to selectively oxidize benzene instead of phenol after generating more active phenol.[8] One promising way to overcome the challenges is to utilize sunlight.[9] Recently, several photocatalytic systems have been developed, including homogeneous,[10] and metal-doped heterogeneous catalysis for the selective hydroxylation of benzene to phenol.[11–13] However, the performance of the current developed photocatalytic systems are unsatisfactory. For the homogeneous catalysts, they cannot be separated from the system themselves. For the metal-doped heterogeneous catalysis, the active species can be leached from the catalysts. The most critical issue is low benzene conversion and poor phenol selectivity. Therefore, there is urgent need to develop new photocatalysts with high efficiency and selectivity.

Inorganic transition-metal compounds, such as Fe, Cu, and V are the most actively studied transition metals for benzene hydroxylation.[14,15] As an organometallic compound, ferrocene has good optical, electric and magnetic properties and redox reversal. Thus, it is widely used in the fields of catalysis, conductors and biology.[16] Compared with inorganic iron ions, ferrocene has rarely been explored in the research of catalyzing direct oxidative hydroxylation reactions.

It was previously reported that the composites of carbon nanotubes (CNTs) and TiO_2 exhibited higher photocatalytic performance than TiO_2 alone.[17,18] Similar to the metals mentioned above, CNTs can also exhibit metal conductivity as one of potential electronic structures. The large electron-storage capacity of CNTs has the ability to accept photon-excited electrons in mixture with titania dioxide or nanocomposites, delaying or hindering recombination.[19] According to this research, CNTs enhance the photoactivity in three different ways (1) act as a sink for electrons to enhance the lifetime of separated charges; (2) serve as a surface impurity incorporation, creating band gap energy states and (3) formation of Ti–O–C or Ti–C defect sites that can absorb visible light and photocatalysis.[20] Hitherto, researches has mainly focused on the CNTs and TiO_2 systems. It is necessary to explore new

[a]*Research Institute of Petroleum Processing, Sinopec, Beijing 100083, P. R. China. E-mail: taozp.ripp@sinopec.com; zhaojie.ripp@sinopec.com*
[b]*University of Chinese Academy of Sciences, Beijing 100049, China*
† These authors contributed equally to this work.

photocatalysis system containing CNTs and expand relevant photocatalytic applications of CNTs. Another unprecedented property of CNTs produces by the fully-sp^2-hybridization and conjugated π-electron system is chemical inertness.[21] It should be noted that chemical inertness does not always contribute to the preparation of these CNTs materials. Due to processability and dispersibility, there are still challenges in various applications, particularly energy-related applications, catalyst supports, and reinforcement of composites.[22] The covalent modification of the graphitic materials is undoubtedly a key to addressing these issues. Many approaches have been utilized for the covalent functionalization of graphitic materials.[23–25] These approaches include the use of radical species, such as aryl intermediates, or oxidization, to react with the surface of CNT or graphene. In almost all instances, the reaction sites can become rehybridized from sp^2 carbon to sp^3 carbon atoms. This alters the exceptional physical properties of the graphitic materials.[26,27] Therefore, a new method is expected to be discovered to disperse the CNT well, but with little or no structural damage to the CNT.

Herein, we synthesized a conjugated microporous polymer (**Fc-POP**) which is based on the Scholl reaction, using ferrocene and 1,3,5-triphenylbenzene as building blocks. In order to obtain higher photocatalytic efficiency and selectivity of benzene hydroxylation, the CNTs were decorated with the **Fc-POP** polymer to obtain the **CNTs@Fc-POP** composites. Additional insight into the photocatalytic benzene hydroxylation to phenol with H_2O_2 over the **Fc-POP** and **CNTs@Fc-POP** has been obtained to prove that the incorporation of CNTs can increase the conversion and selectivity of phenol.

Experimental

Materials and methods

Ferrocene, $AlCl_3$ and 1,3,5-triphenylbenzene (*sym*-$PhPh_3$) were commercially available and purchased from Alfa Aesar. The multi-walled carbon nanotubes (MWCNT) were purchased from Heng Qiu Science and Technology Ltd. The length of the MWCNT is 3–12 μm and the diameter is 8–15 nm. All the reagents were analytical grade and used without further purification.

Synthesis of TPB

sym-$PhPh_3$ (1.44 g, 5 mmol), chloroform (15 mL) and $AlCl_3$ (4.82 g, 30 mmol) were sequentially added to a 50 mL round bottom flask. The resultant mixture was stirred under N_2 atmosphere for 15 min and then refluxed for 48 h. After the mixture cooled to room temperature, methanol (30 mL) was added to stir for another 1 h. The resulting precipitate was collected by filtration and the solid was washed three times with water, ethanol and tetrahydrofuran (THF). The powder was abstracted with alcohol in a Soxhlet extractor for 24 h and dried in a vacuum oven at 75 °C for 12 h to get final product (pale brown powder, 99% yield).

Synthesis of Fc-POP

sym-$PhPh_3$ (0.918 g, 3 mmol), ferrocene (n(*sym*-$PhPh_3$) : n(Fc) = 3 : 1, 2 : 1, or 3 : 2) chloroform (15 mL) and $AlCl_3$ (4.82 g, 30 mmol) were sequentially added to a 50 mL round bottom flask. The resultant mixture was stirred under N_2 atmosphere for 15 min and then refluxed for 48 h. After the mixture cooled to room temperature, methanol (50 mL) was added to stir for another 1 h. The resulting precipitate was filtered and washed three times with HCl–H_2O (v/v = 2 : 1), ethanol and THF. The powder was further abstracted with alcohol in a Soxhlet extractor for 24 h and then dried in a vacuum oven at 75 °C for 12 h to get final product (dark black powder, 75% yield).

Synthesis of Fc-CNT-POP

sym-$PhPh_3$ (0.918 g, 3 mmol), multi-wall nanotubes (0.2 g), 25 mL of chloroform, and ferrocene (0.372 g, 2 mmol) were sequentially added to a 50 mL round bottom flask. The resultant mixture was stirred under N_2 atmosphere for 2 min before $AlCl_3$ (4.82 g, 30 mmol) was added to it, and then refluxed for 48 h. After cooling to room temperature, 50 mL of methanol was added into the mixture to stir for 1 h. After filtration and washing three times with HCl–H_2O (v/v = 2 : 1), ethanol and THF, the obtained powder was abstracted with alcohol in a Soxhlet extractor for 24 h. The final solid was dried in a vacuum oven at 75 °C for 12 h (dark black powder, 99% yield).

Instrumental characterization and structural analysis

Solid-state cross-polarization magic angle spinning (CP/MAS) NMR spectra of the polymers and composite were obtained on a Bruker Avance III 400 Nuclear Magnetic Resonance (NMR) spectrometer (Bruker Daltonics Inc., Switzerland). The infrared (IR) spectra were obtained from a Fourier transform infrared (FTIR) spectrometer (PerkinElmer, USA). Transmission Electron Microscope (TEM) observations were obtained using a Tecnai G^2 20 S-TWIN microscope (FEI, USA) at the accelerating voltage of 200 kV. Nitrogen sorption–desorption isotherm was measured at 77 K using a Micromeritics 2020M + C system after the sample was degassed at 120 °C overnight and the surface areas were determined by Brunauer–Emmett–Teller(BET) method. (Micromeritics Instrument Corporation, USA). The Pore Size Distribution (PSD) was calculated by Non-local density functional theory (NLDFT). Electron paramagnetic resonance (EPR) measurements were carried out on a Bruker model A300 spectrometer with a 300 W Xenon lamp. All Gas Chromatography (GC) experiments were carried out and recorded with a SHIMADZU GC-2010 with flame ionization detector (FID) detector.

Photocatalytic reaction

The general experimental procedure for the hydroxylation of benzene was carried out as following and detailed conditions are presented in Table 2. Benzene (0.2 mL) and photocatalyst (50 mg) were added in a mixture of acetonitrile (4 mL) and water (4 mL). After ultrasonic treatment for 15 min, the catalyst was dispersed evenly. Then hydrogen peroxide (30 wt%, 0.8 mL, 8 mmol) was slowly added into the stirring mixture, following by irradiation for 4 h with a 300 W Xenon light. The reaction was quenched with 9.6 mL of ethanol and the heterogenous catalyst was separated by filter membrane. GC was employed to

qualitatively analyze the filtrate and standard chemicals were used to determine the conversion and selectivity of phenols.

Results and discussion

Referring to the previous research from Tan *et al.*,[28] the conjugated microporous polymers (**Fc-POP**) were synthesized though the Scholl reaction which involved the coupling reaction between two aromatic molecules and accompanied by the formation of a new aryl–aryl (as shown in Scheme 1). Acting as light backbones, 1,3,5-triphenylbenzene guarantees the porosity and specific surface area whilst its fluorescence enhances the photo-catalytic properties of the polymers. Ferrocene acts as active site in the reaction of benzene hydroxylation to phenol. Different from the physical incorporation heterogeneous catalysis, the active species were uniformly distributed and connected to the skeleton by covalent bond that can avoid leaching and losing themselves.

In order to synthesize **Fc-POP** with different ferrocene contents, different molar ratio of *sym*-$PhPh_3$ and ferrocene: *n*(*sym*-$PhPh_3$)/*n*(ferrocene) = 3/1, 2/1 or 3/2 was added before the reaction started and the final polymers were named after **FC-POP1**, **FC-POP2** and **FC-POP3** respectively. All obtained polymers are chemically stable, even when exposed to HCl or NaOH solution.

The structures of these polymers were confirmed at molecular level by a FTIR spectrometer and ^{13}C CP/MAS NMR spectrometer. A comparison of FTIR spectra of the polymers is shown in Fig. 1. The weak peaks near 3000 cm^{-1} are attributed to C–H stretching in the aromatic rings; peaks near 1650 cm^{-1}, 1600 cm^{-1} and 1450 cm^{-1} are attributed to the benzene ring skeleton vibrations; the peak at 1050 cm^{-1} is attributed to the cyclopentadiene rings skeleton vibrations. It can be inferred from the spectra that the conjugated microporous polymers (**Fc-POP**) were successfully synthesized and they are consistent with the proposed structure. However, the same wave numbers and transmittance of characteristic peaks can be found in the three FT-IR spectra of **Fc-POP1–3**. It indicates that the structure and ferrocene content of these three polymers are almost same. If ferrocene was incorporated with various ratios, the peak intensity of benzene rings and cyclopentadienyl rings should differ from each other.

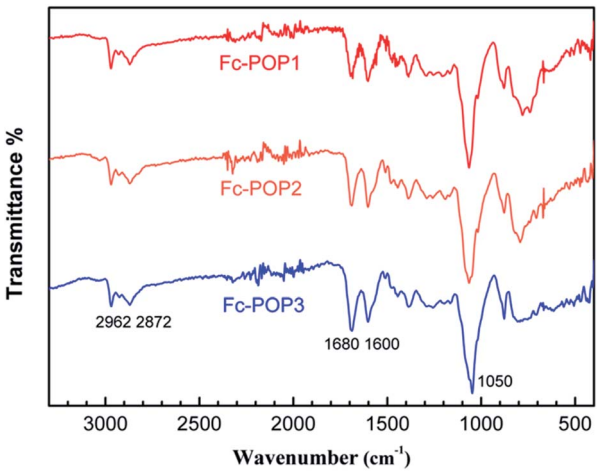

Fig. 1 FT-IR spectra of **Fc-POP1–3**.

The ^{13}C CP/MAS NMR spectra of the three polymers are shown in Fig. 2. These polymers show the almost the same spectra. The peaks at 140 and 128 ppm are ascribed to the coupling of benzene carbons and noncoupling benzene carbons respectively. While the peaks at 80 and 67 ppm are corresponded to the coupling of ferrocene carbons and noncoupling ferrocene carbons respectively. The peaks around 14 and 57 ppm of all samples are assigned to the carbons of remaining ethanol adsorbed in the micropores or ultra-micropores, which is consistent with published reports.[28] As the micropores or ultra-micropores are very small, there is usually some solvent molecules left in the materials, which is hard to completely remove even after drying in a vacuum oven.[29] In all the three ^{13}C CP/MAS NMR spectra, the peaks intensities at 80 and 67 ppm are low and almost the same. The result are consistent with the FTIR spectra, indicating that the three polymers contain the same amount of incorporated ferrocene. Our initial goal to obtain different ferrocene-incorporated conjugated

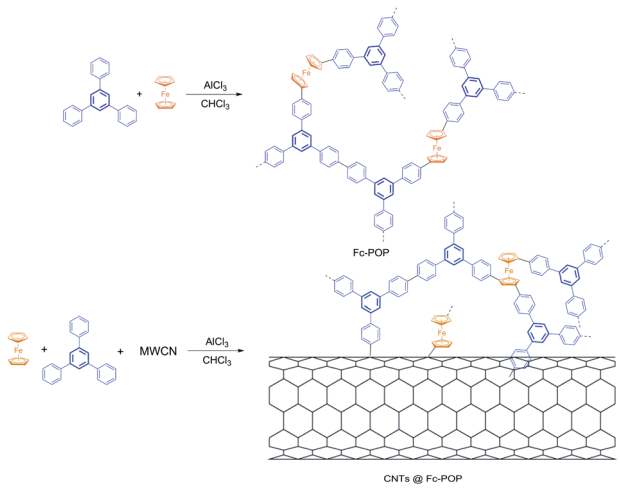

Scheme 1 Preparation of the **Fc-POP** and **CNTs@Fc-POP**.

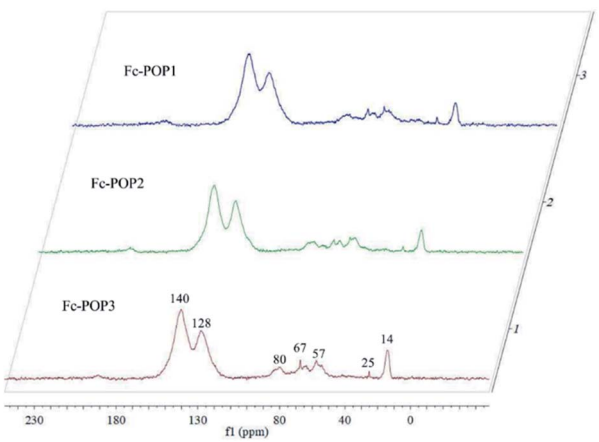

Fig. 2 ^{13}C CP/MAS NMR spectra of **Fc-POP1–3**.

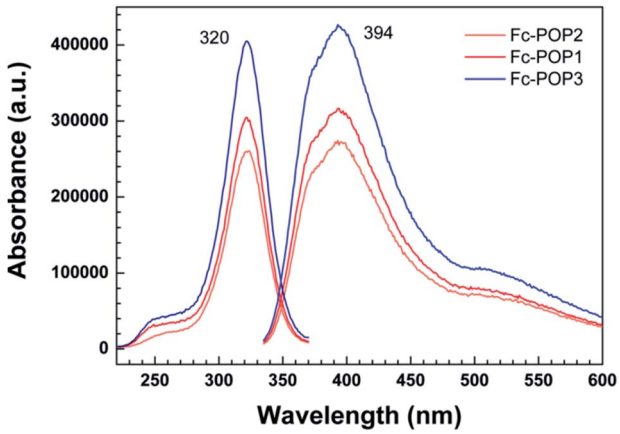

Fig. 3 Excitation and emission spectra of **Fc-POP1–3**.

microporous polymers was not realized, which might be due to the lower reactivity of ferrocene in the Scholl reaction. Regardless of the amount of ferrocene added, only a small certain portion was incorporated into the polymers.

The excitation and emission spectra of the three materials (**Fc-POP1**, **Fc-POP2** and **Fc-POP3**) were tested, as shown in Fig. 3. It can be seen that the three polymers have the same maximum excitation and occurrence wavelength, but the intensity is slightly different. Their maximum excitation wavelength is about 320 nm and the maximum emission wavelength is about 390 nm, proving that the material we obtained is a fluorescent solid material, which plays an important role in direct photocatalytic benzene hydroxylation to phenol.

The porosity of the **Fc-POP**s was also analyzed by N_2 sorption analysis. The nitrogen adsorption–desorption isotherms of the three polymers at 77 K are displayed in Fig. 4 and the characterization data such as the surface area and pore volume are summarized in Table 1. According to the IUPAC classification, the adsorption–desorption isotherms are all categorized into type I. In low pressure range ($P/P_0 < 0.001$), the isotherms show an obvious rising trend, indicating an extensive micropores structure. Additionally, hysteresis loops were observed in the entire relative pressure range extending to the lowest attainable pressures, which is due to the irreversible uptake of gas molecules in the pores (or through pore entrances) with the same diameter as that of N_2 molecule.[30] Using the five adsorption points in 0.01–0.1 relative pressure, the BET specific surface areas of **Fc-POP1–3** were measured to be 1320, 1200 and 1360 $m^2\ g^{-1}$ respectively, showing very little difference. This further demonstrates the conclusion from IR and NMR that almost the same amount of ferrocene was incorporated in these three materials. The pore distribution (Fig. 4) of **Fc-POP1–3** indicates that they possess ultra-micropores (smaller than 0.7 nm). Compared to the previously reported MOPs, **Fc-POP1–3** possess smaller pores in the micropore region, with a relatively narrow pore size distribution and no obvious peaks beyond 2 nm in the pore size distribution.

Considering the highest specific surface area and best fluorescence, **Fc-POP3** was chose to investigate the catalytic activity for the benzene hydroxylation reaction. Using H_2O_2

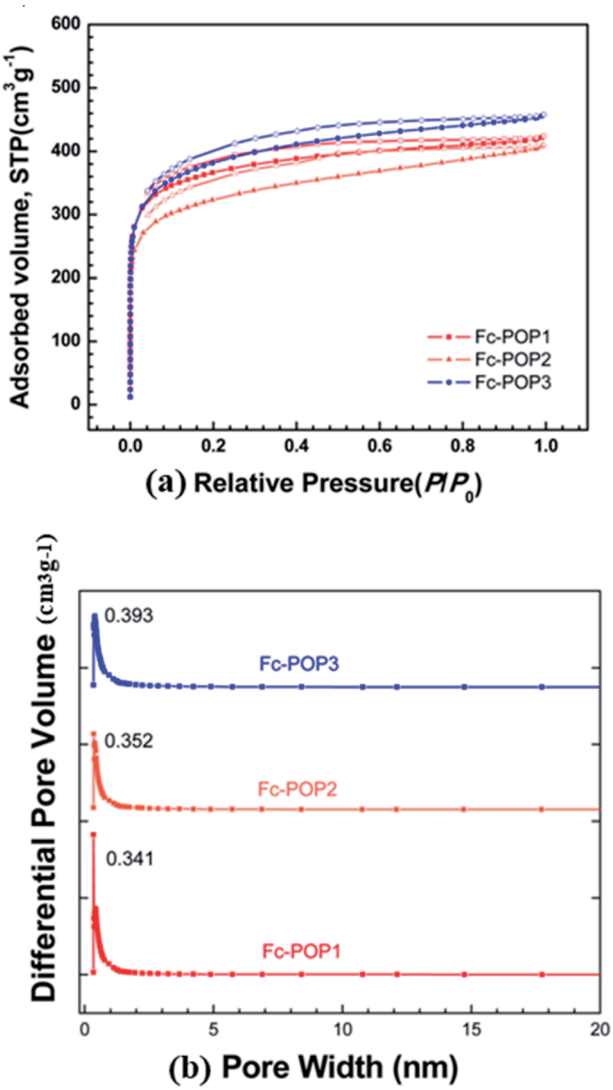

Fig. 4 (a) Nitrogen adsorption–desorption isotherms of **Fc-POP1–3** measured at 77 K, the adsorption and desorption branches are labeled with solid and open symbols, respectively. (b) The PSD profiles of **Fc-POP1–3** calculated by NLDFT.

(H_2O_2 : benzene ratio of 3 : 4) as cocatalyst and oxidant, xenon light as the photon source, the benzene hydroxylation reaction was initially conducted in acetonitrile (CH_3CN). It was found that **Fc-POP3** can effectively hydroxylate benzene to phenol under this condition. As shown in Table 2, entries 2 and 3, the control experiments without ferrocene or light irradiation achieved very low or even undetectable products, indicating the light irradiation and ferrocene are essential for the reaction and the hydroxylation of benzene to phenol over **Fc-POP3**.

Solvent plays an important role in this reaction. According to the research about the solvents investigated, a CH_3CN/H_2O mixed solvent 1 : 1 (v/v) gave the best performance by showing the highest benzene conversion ratio.[31] So the mixture solvent was used in our catalytic system to find out the effect on the reaction. Comparing entries 1 and 4 in Table 2, the reaction conducted in the mixed solvent is more effective in benzene

Table 1 Porosity properties of Fc-POP1–3

Polymers	S_{BET}[a] ($m^2\ g^{-1}$)	S_{micro}[b] ($m^2\ g^{-1}$)	V_{total}[c] ($cm^3\ g^{-1}$)	D_{pore}[d] (nm)
Fc-POP1	1326	1153	0.64	0.393
Fc-POP2	1164	937	0.62	0.352
Fc-POP3	1361	1130	0.70	0.341

[a] Specific surface area calculated from the nitrogen adsorption isotherm using the BET method. [b] Micropore surface area calculated from the adsorption branch of the nitrogen adsorption–desorption isotherm using the *t*-plot method. [c] Total pore volume at $P/P_0 = 0.99$. [d] Data calculated from nitrogen adsorption isotherms with the NLDFT method.

Table 2 Photocatalytic benzene hydroxylation to form phenol over Fc-POP3

Entry	Catalyst (*x* mg)	Light source	Solvent	V_{ben} (mL)	Yield (%)
1	**Fc-POP3** (25)	Xe lamp	Acetonitrile	0.8	2.7
2	**Fc-POP3** (25)	Dark	Acetonitrile	0.8	0.3
3	TPB (25)	Xe lamp	Acetonitrile	0.8	—
4	**Fc-POP3** (25)	Xe lamp	Mixture	0.8	5.2
5	**Fc-POP3** (50)	Xe lamp	Mixture	0.1	9.4
6	**Fc-POP3** (50)	Xe lamp	Mixture	0.4	13.1
7	**Fc-POP3** (50)	Xe lamp	Mixture	0.8	18.1

hydroxylation, and the phenol production (5.2%) is almost twice than that in bare CH_3CN (2.7%). After further optimization of the benzene concentration and catalyst loading, the best yield of phenol can reach 18.1%. All the yield of phenol is calculated by using GC.

Recently, carbon nanotubes were introduced to TiO_2 photocatalysts and the resultant composite catalyst showed very good activity on oxidation of organic compounds. It was the synergistic effect between TiO_2 and carbon nanotubes that promoted the transmittance of photo-generated electrons from the former to the latter, consequently prolonging the life of photo-generated electron–hole pairs and granting the composite catalyst the ability to absorb visible light. In order to find out whether the CNTs possess the similar synergistic effect in our catalytic system and whether it can enhance the product yield, we tried to combine our porous **Fc-POP** with CNTs. The defect/edge-selective functionalization protocol is an attractive and versatile alternative used in various nanocarbon functionalization strategies.[32] Compared with other functionalization systems, defect/edge-selective functionalization is benign enough not to damage graphitic frameworks. Thus, it allows preservation of the intrinsic properties of graphitic materials. Friedel–Crafts acylation reaction has been used for the defect/edge-selective functionalization of carbon materials.[33] Considering the similar reaction mechanism and condition between the Friedel–Crafts acylation reaction and Scholl reaction, we tried to modify the **Fc-POP** into WMCNTs through the defect/edge-selective functionalization method.

The composite of **Fc-POP** and MWCNTs (**CNTs@Fc-POP**) was successfully synthesized just *via* adding some MWCNTs into the ferrocene and *sym*-PhPh3 solution and stirring several hours before the polymerization reaction. The FT-IR spectrum and ^{13}C CP/MAS NMR spectrum of **CNTs@Fc-POP** are shown in Fig. 5 and Fig. 6. Due to the π–π interaction between the MWCNTs and reactive molecules (ferrocene and *sym*-PhPh3), these molecules stack on the surface of the MWCNTs and can react with the defect/edge sites (mostly sp^2 C–H) of MWCNTs, the polymer shell will be fabricated and coated with the MWCNTs after the polymerization reaction.

From the representative TEM images of **CNTs@Fc-POP** and MWCNTs shown in Fig. 7, it can be seen that the obtained composite which has one-dimension tubular structure. The MWCNTs with about 12 nm mean diameter are individually coated with the uniform gray polymer shell with a thickness of about 10 nm. This demonstrates the successful synthesis of a novel MWCNTs composite through a facile method.

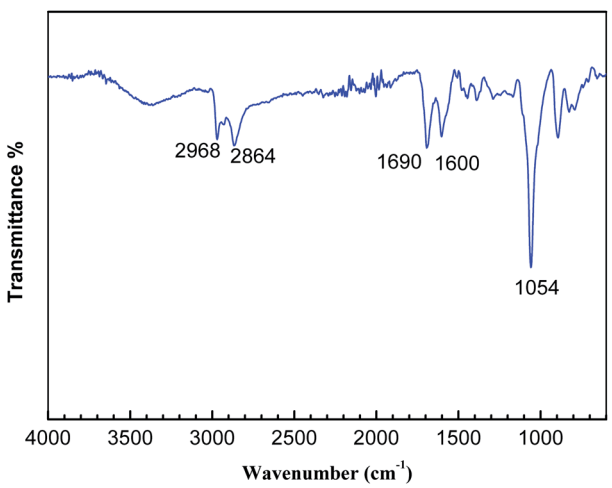

Fig. 5 FT-IR spectra of CNTs@Fc-POP.

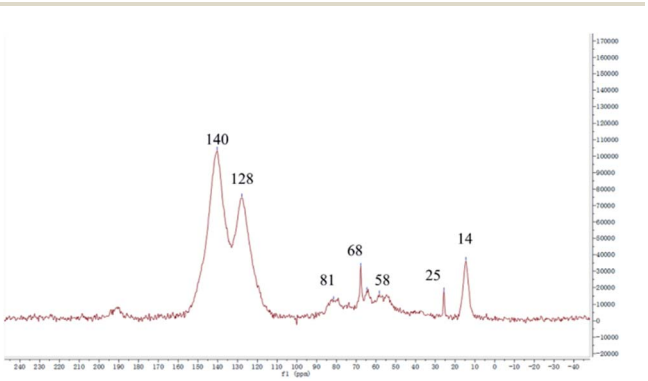

Fig. 6 ^{13}C CP/MAS NMR spectra of CNTs@Fc-POP.

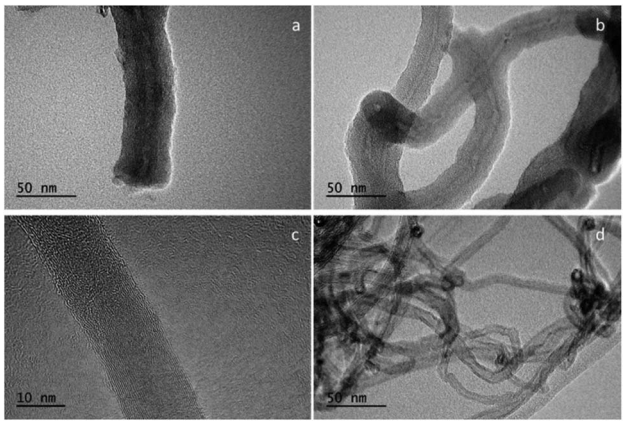

Fig. 7 TEM images of CNTs@Fc-POP (a and b) and MWCNTs (c and d).

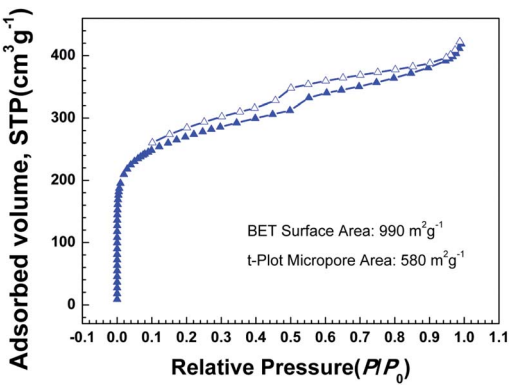

Fig. 8 Nitrogen adsorption–desorption isotherms of CNTs@Fc-POP measured at 77 K, the adsorption and desorption branches are labeled with solid and open symbols, respectively.

The nitrogen adsorption–desorption isotherms of **CNTs@Fc-POP** at 77 K are displayed in Fig. 8. Compared with the isotherms of **Fc-POP**s with almost no change of adsorption quantity in the media and high pressure range, there is an obvious increase of **CNTs@Fc-POP** isotherms in this range. **Fc-POP**s possess a relatively narrow pore size distribution and no obvious peaks beyond 2 nm in the pore size distribution, while the micropores specific surface area of **CNTs@Fc-POP** is 580 $m^2 g^{-1}$, 60% of the total. Because of the combination of MWCNTs, the rest 40% was attributed to meso- and macro-pores. For heterogeneous catalysts, porosity is beneficial to the catalytic process: a large specific surface area can help the full mixing of reactants and catalytic sites. Apart from this, meso- and macro-pores accelerate the mass transfer rates of reactants and products.

The catalytic activity of the **CNTs@Fc-POP** in hydroxylation of benzene was investigated under the same conditions as **Fc-POP** (Table 3). The highest yield was improved to 25.3%. We also examined the recyclability of the heterogeneous photocatalysts. The catalysts were recycled by centrifugation. The recovered catalyst was repeatedly used after being dried overnight in vacuum, and no obviously deterioration of conversion is determinated for the reaction after three times of benzene hydroxylation.

Table 3 Photocatalytic benzene hydroxylation to form phenol over CNTs@Fc-POP

Entry	Catalyst (x mg)	Light source	Solvent	V_{ben} (mL)	Yield (%)
1	**Fc-POP3** (50)	Xe lamp	Mixture	0.8	18.1
2	**CNTs@Fc-POP** (50)	Xe lamp	Mixture	0.8	25.3
3	Recycle-1	Xe lamp	Mixture	0.8	24.2
4	Recycle-2	Xe lamp	Mixture	0.8	23.8
5	Recycle-3	Xe lamp	Mixture	0.8	24.1
6	**CNTs@Fc-POP** (50)	Dark	Mixture	0.8	0.2

The chemical stability of photocatalyst was evaluated after long term test. The catalytic activity of the **CNTs@Fc-POP** in hydroxylation of benzene was investigated over 26 h. The best yield of phenol can reach 25.3% at 4 h, while the yield was decreased after 4 h due to the increase of byproducts. The TEM and ICP were used to characterize the chemical stability of **CNTs@FC-POP** after 26 h. It was observed that the MWCNTs are still coated with the uniform polymer shell with a thickness of about 10 nm after the long term reaction. The structure was not damaged, but the surface becomes a little irregular. The material **CNTs@Fc-POP** is also characterized *via* ICP-OES after reaction. It has been observed that the content of Fe is 4.8% after a long term reaction, while the content is 4.9% before reaction, meaning that the catalyst is stable enough over a long periods of time.

The excellent performance was attributed to the following reasons: (1) carbon nanotubes have a large amount of unpaired electrons on the wall which make carbon nanotubes have the properties of both metals and semi-conductors and thus promote the surface photocatalysis which is governed by electron transmission; (2) carbon nanotubes have good capacity to store electrons and can receive the photo-excited electrons from polymer shell and inhibit the combination of photogenerated electron–hole pairs; (3) the addition of carbon nanotubes introduced meso-pores and macro-pores, which accelerate the mass transfer rates of reactants and products. Compared with other reported heterogeneous catalysts using Fe as active site (as

Table 4 Catalytic activity of various Fe-based composite for benzene hydroxylation

Materials	S_{BET}[a] ($m^2 g^{-1}$)	Yield of phenol (%)	Ref.
CNTs@Fc-POP	990	25	This work
5.0Fe/NACH-600N	600	20	34
AlFePO (0.02)450	248	22	35
SBA-15-N = ferrocene	658	15	16
Fe–CN/TS-1	266	10	36
Fe/MWCNTs	216	11	37
MIL-100 (Fe)	—	22	38
Fc-MCN	51	14	39
Fe-g-C_3N_4/SBA-15	451	12	40

[a] Specific surface area calculated from the nitrogen adsorption isotherm using the BET method.

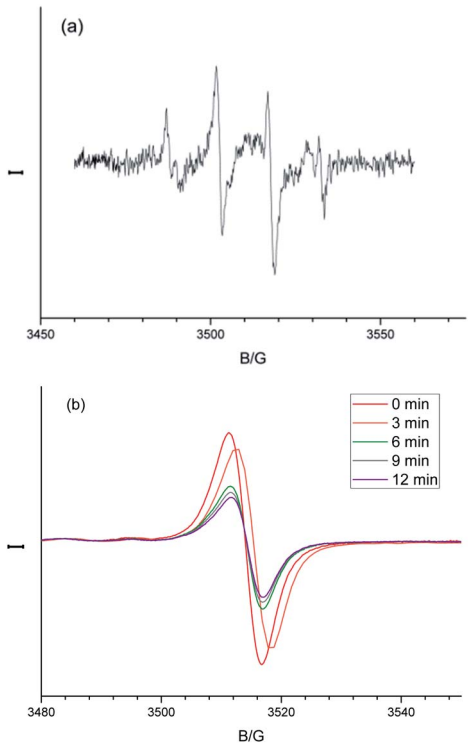

Fig. 9 (a) The DMPO spin-trapping ESR spectra for the ·OH radical in the mixture of **CNTs@Fc-POP** hybrids (50 mg) and 30% wt H_2O_2 (0.4 mL) in CH_3CN (8 mL) under light irradiation. (b) The Fe^{3+} ESR spectra of **CNTs@Fc-POP** as time go on.

shown in Table 4), our catalysts performed the highest yield. Furthermore, they have the advantages of simple synthesis, mild reaction conditions and cheap starting materials.

To further understand the catalysed benzene oxidation, we moved forward the mechanism investigation. The benzene hydroxylation to produce phenol by H_2O_2 is generally believed to proceed *via* an oxygenation pathway induced by the *in situ*-formed ·OH. When ethanol (1 mL), a ·OH radical scavenger, was added into the oxidation of benzene, no oxidation occurred anymore, indicating that the oxidation may follow a pathway through the ·OH radical-induced benzene hydroxylation. Moreover, when the photolysis of H_2O_2 was performed in the presence of the **CNTs@Fc-POP** composite, the formation of ·OH was confirmed by electron spin resonance (ESR) and DMPO (5,5-dimethyl-1-pyrrolineN-oxide) spin-trapping technique, as the signal for the DMPO-··OH additive was observed on the ESR spectra (Fig. 9a).

In most case, the ·OH radicals are generated under Fenton like conditions ($Fe^{2+} + H_2O_2 \rightarrow Fe^{3+} + \cdot OH + OH^-$) and the regeneration of Fe^{2+} (by reduction of Fe^{3+} to Fe^{2+}) is the key step in the catalytic cycle. It is reasonable to consider that the electrons from the MWCNTs of **CNTs@Fc-POP** can possibly reduce the Fe^{3+} to Fe^{2+} for H_2O_2 activation. To test this hypothesis, we used the ESR measurements to study the reduction process. Only Fe^{3+} with $3d^5$ structure affords a single peak signal on the spectra, while Fe^{2+} shows no clear response in the ESR spectra. So the peak intensity of the ESR signal is proportional to the concentration of unpaired electrons (Fe^{3+}) in the sample and

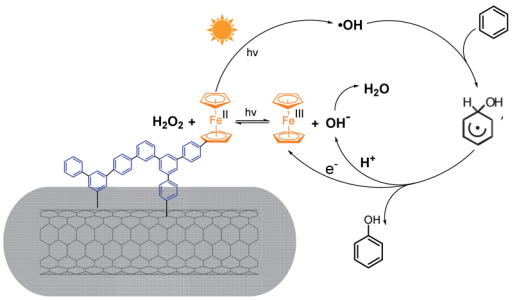

Scheme 2 Possible reaction mechanism for the photocatalytic benzene hydroxylation over **CNTs@Fc-POP**.

the decreasing intensity can be used to value the Fe^{3+} concentration change. Interestingly, when testing **CNTs@Fc-POP** under light illumination, a gradual decrease of Fe^{3+} signal was observed over time, which directly proves that the photo-excited electrons can reduce the Fe^{3+} to Fe^{2+} in the system (Fig. 9b).

P. W. Cyr[41,42] reported that irradiation of thin films of poly (ferrocenylmethylphenylsilane) ([Fe(η^5-C_5H_4)$_2$SiMePh]n) cast from chloroform solution with UV light leads to photooxidation of ferrocene centers in the polymer main chain, indicating that the ferrocene is photo-active. The control experiments were also conducted using the ferrocene as catalyst in dark and under illumination conditions respectively. The yield of phenol is only 0.3% in dark condition while the yield can be 8.2% under illumination condition, also proving the photo-active role of ferrocene.

On the basis of the observations described above, the mechanism for photocatalytic benzene hydroxylation to phenol over **CNTs@Fc-POP** was proposed (Scheme 2). The light-trigged catalytic cycle starts with the reaction of Fc(II) and H_2O_2 to produce a hydroxyl radical (·OH), OH^- and Fc(III) ($Fe^{2+} + H_2O_2 \rightarrow Fe^{3+} + \cdot OH + OH^-$). The ·OH radical attacks the aromatic ring, followed by dimerization of the resulting hydroxycyclohexadienyl radicals. Subsequently, the hydroxycyclohexadienyl radicals donate an electron to Fc(III) to achieve regeneration of Fc(II) and yield phenol, while releasing H^+ to react with OH^- to produce H_2O. Then, the regenerated Fc(II) reacts with H_2O_2 to restart the catalytic cycle.

Conclusions

By using ferrocene and *sym*-Ph_3Ph as building blocks, we synthesized ferrocene-incorporated conjugated micropores polymer (**Fc-POP**). To increase its photo-catalytic properties, we synthesized novel carbon-organic composite **CNTs@Fc-POP**. These two kinds of materials can be used as heterogeneous catalysts, and their catalytic activity was studied within the context of hydroxylation of benzene to phenol. Both of them show very better activities than reported catalysts, and the yields are 18.1% and 25.3%, respectively.

Conflicts of interest

There are no conflicts to declare.

Acknowledgements

The financial support of National Natural Science Foundation of China (Grant No. 21272263), National key research and development plan (2016YFF0203700) is acknowledged.

References

1 T. Dong, J. Li, F. Huang, L. Wang, J. Tu, Y. Torimoto, M. Sadakata and Q. X. Li, *Chem. Commun.*, 2005, **21**, 2724.
2 H. Hock and S. Lang, *Ber. Dtsch. Chem. Ges.*, 1944, **77**, 257.
3 Y.-Y. Gu, X.-H. Zhao, G.-R. Zhang, H.-M. Ding and Y.-K. Shan, *Appl. Catal., A*, 2007, **328**, 150.
4 bS. S. Acharyya, S. Ghosh, R. Tiwari, C. Pendem, T. Sasaki and R. Bal, *ACS Catal.*, 2015, **5**, 2850.
5 I. Yuranov, D. A. Bulushev, A. Renken and L. Kiwi-Minsker, *Appl. Catal., A*, 2007, **319**, 128.
6 Y. Li, Z. Feng, R. A. van Santen, E. J. M. Hensen and C. Li, *J. Catal.*, 2008, **255**, 190.
7 B. Guo, L. Zhu, X. Hu, Q. Zhang, D. Tong, G. Li and C. Hu, *Catal. Sci. Technol.*, 2011, **1**, 1060.
8 C. I. Herrerias, X. Yao, Z. Li and C.-J. Li, *Chem. Rev.*, 2007, **107**, 2546.
9 H. Tong, S. Ouyang, Y. Bi, N. Umezawa, M. Oshikiri and J. Ye, *Adv. Mater.*, 2012, **24**, 229.
10 P. T. Tanev, M. Chibwe and T. J. Pinnavaia, *Nature*, 1994, **368**, 321.
11 K. Ohkubo, T. Kobayashi and S. Fukuzumi, *Angew. Chem., Int. Ed.*, 2011, **50**, 8652.
12 K. Ohkubo, A. Fujimoto and S. Fukuzumi, *J. Am. Chem. Soc.*, 2013, **135**, 5368.
13 P. Devaraji, N. K. Sathu and C. S. Gopinath, *ACS Catal.*, 2014, **4**, 2844.
14 G. Tanarungsun, W. Kiatkittipong, P. Praserthdam, H. Yamada, T. Tagawa and S. Assabumrungrat, *J. Ind. Eng. Chem.*, 2008, **14**, 596.
15 J. S. Choi, T. H. Kim, K. Y. Choo, J. S. Sung, M. B. Saidutta, S. D. Song and Y. W. Rhee, *J. Porous Mater.*, 2005, **12**, 301.
16 D. R. Burri, I. R. Shaikh, K.-M. Choi and S.-E. Park, *Catal. Commun.*, 2007, **8**, 731.
17 Y. Zhang, Z. R. Tang, X. Fu and Y. J. Xu, *ACS Nano*, 2010, **4**, 7303.
18 B. K. Vijayan, N. M. Dimitrijevic, D. Finkelstein-Shapiro, J. Wu and K. A. Gray, *ACS Catal.*, 2012, **2**, 223.
19 A. Kongkanand and P. V. Kamat, *ACS Nano*, 2007, **1**, 13.
20 K. Woan, G. Pyrgiotakis and W. Sigmund, *Adv. Mater.*, 2009, **21**, 2233.
21 A. Hirsch, *Nat. Mater.*, 2010, **9**, 868.
22 A. Hirsch, *Angew. Chem., Int. Ed.*, 2002, **41**, 1853.
23 D. Tasis, N. Tagmatarchis, A. Bianco and M. Prato, *Chem. Rev.*, 2006, **106**, 1105.
24 V. Georgakilas, M. Otyepka, A. B. Bourlinos, V. Chandra, N. Kim, K. C. Kemp, P. Hobza, R. Zboril and K. S. Kim, *Chem. Rev.*, 2012, **112**, 6156.
25 S. Eigler and A. Hirsch, *Angew. Chem., Int. Ed.*, 2014, **53**, 7720.
26 E. Bekyarova, S. Sarkar, F. Wang, M. E. Itkis, I. Kalinina, X. Tian and R. C. Haddon, *Acc. Chem. Res.*, 2013, **46**, 65.
27 A. Ciesielski and P. Samor, *Adv. Mater.*, 2016, **28**, 6030.
28 B. Li, Z. Guan, X. Yang, W. D. Wang, W. Wang, I. Hussain, K. Song, B. Tan and T. Li, *J. Mater. Chem. A*, 2014, **2**, 11930.
29 S. Ren, M. J. Bojdys, R. Dawson, A. Laybourn, Y. Z. Khimyak, D. J. Adams and A. I. Cooper, *Adv. Mater.*, 2012, **24**, 2357.
30 K. S. W. Sing, D. H. Everett, R. A. W. Haul, L. Moscou, R. A. Pierotti, J. Rouquerol and T. Siemieniewska, *Pure Appl. Chem.*, 1985, **57**, 603.
31 D. Bianchi, R. Bortolo, R. Tassinari, M. Ricci and R. Vignola, *Angew. Chem., Int. Ed.*, 2000, **39**, 4321.
32 Z. Xiang, Q. Dai, J.-F. Chen and L. Dai, *Adv. Mater.*, 2016, **28**, 6253.
33 J. M. Seo, L. S. Tan and J. B. Baek, *Adv. Mater.*, 2017, **29**, 1606317.
34 J. S. Choi, T. H. Kim, K. Y. Choo, J. S. Sung, M. B. Saidutta, S. O. Ryu, S. D. Song, B. Ramachandra and Y. W. Rhee, *Appl. Catal., A*, 2005, **290**, 1.
35 R. Navarro, S. Lopez-Pedrajas, D. Luna, J. M. Marinas and F. M. Bautista, *Appl. Catal., A*, 2014, **474**, 272.
36 X. Ye, Y. Cui, X. Qiu and X. Wang, *Appl. Catal., B*, 2014, **383**, 152.
37 S. Song, H. Yang, R. Rao, H. Liu and A. Zhang, *Appl. Catal., A*, 2010, **375**, 265.
38 D. Wang, M. Wang and Z. Li, *ACS Catal.*, 2015, **5**, 6852.
39 X. Ye, Y. Cui and X. Wang, *ChemSusChem*, 2014, **7**, 738.
40 X. Chen, J. Zhang, X. Fu, M. Antonietti and X. Wang, *J. Am. Chem. Soc.*, 2009, **131**, 11658.
41 P. W. Cyr, M. Tzolov, I. Manners and E. H. Sargent, *Macromol. Chem. Phys.*, 2003, **204**, 915.
42 P. W. Cyr, E. J. D. Klem, E. H. Sargent and I. Manners, *Chem. Mater.*, 2005, **17**, 5770.